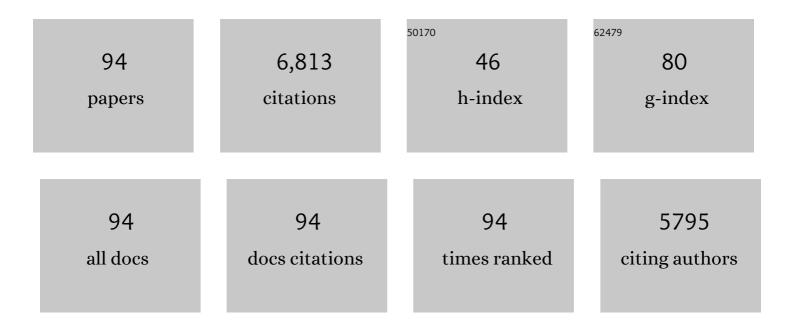
Silvia Spinelli

List of Publications by Year in descending order

Source: https://exaly.com/author-pdf/11307907/publications.pdf Version: 2024-02-01



SILVIA SDINFLLL

#	Article	IF	CITATIONS
1	Conformations of immunoglobulin hypervariable regions. Nature, 1989, 342, 877-883.	13.7	1,199
2	Biogenesis and structure of a type VI secretion membrane core complex. Nature, 2015, 523, 555-560.	13.7	241
3	Mammalian odorant binding proteins. BBA - Proteins and Proteomics, 2000, 1482, 229-240.	2.1	234
4	Domain swapping creates a third putative combining site in bovine odorant binding protein dimer. Nature Structural and Molecular Biology, 1996, 3, 863-867.	3.6	194
5	Directed in Vitro Evolution and Crystallographic Analysis of a Peptide-binding Single Chain Antibody Fragment (scFv) with Low Picomolar Affinity. Journal of Biological Chemistry, 2004, 279, 18870-18877.	1.6	160
6	A common protein fold and similar active site in two distinct families of β-glycanases. Nature Structural Biology, 1995, 2, 569-576.	9.7	149
7	Three Camelid VHH Domains in Complex with Porcine Pancreatic α-Amylase. Journal of Biological Chemistry, 2002, 277, 23645-23650.	1.6	145
8	Camelid Heavy-Chain Variable Domains Provide Efficient Combining Sites to Haptensâ€. Biochemistry, 2000, 39, 1217-1222.	1.2	144
9	Complexes of porcine odorant binding protein with odorant molecules belonging to different chemical classes. Journal of Molecular Biology, 2000, 300, 127-139.	2.0	139
10	Crystal structure of Apis mellifera OBP14, a C-minus odorant-binding protein, and its complexes with odorant molecules. Insect Biochemistry and Molecular Biology, 2012, 42, 41-50.	1.2	135
11	The crystal structure of a llama heavy chain variable domain. Nature Structural and Molecular Biology, 1996, 3, 752-757.	3.6	131
12	Priming and polymerization of a bacterial contractile tail structure. Nature, 2016, 531, 59-63.	13.7	127
13	The Structure of the Monomeric Porcine Odorant Binding Protein Sheds Light on the Domain Swapping Mechanism‡. Biochemistry, 1998, 37, 7913-7918.	1.2	126
14	Structure of the phage TP901-1 1.8ÂMDa baseplate suggests an alternative host adhesion mechanism. Proceedings of the National Academy of Sciences of the United States of America, 2012, 109, 8954-8958.	3.3	121
15	Lactococcal bacteriophage p2 receptor-binding protein structure suggests a common ancestor gene with bacterial and mammalian viruses. Nature Structural and Molecular Biology, 2006, 13, 85-89.	3.6	117
16	Receptor-Binding Protein of Lactococcus lactis Phages: Identification and Characterization of the Saccharide Receptor-Binding Site. Journal of Bacteriology, 2006, 188, 2400-2410.	1.0	116
17	The Crystal Structure of a Cockroach Pheromone-binding Protein Suggests a New Ligand Binding and Release Mechanism. Journal of Biological Chemistry, 2003, 278, 30213-30218.	1.6	115
18	Isolation of Llama Antibody Fragments for Prevention of Dandruff by Phage Display in Shampoo. Applied and Environmental Microbiology, 2005, 71, 442-450.	1.4	113

#	Article	IF	CITATIONS
19	Crystal Structure of the Open Form of Dog Gastric Lipase in Complex with a Phosphonate Inhibitor. Journal of Biological Chemistry, 2002, 277, 2266-2274.	1.6	107
20	Modular Structure of the Receptor Binding Proteins of Lactococcus lactis Phages. Journal of Biological Chemistry, 2006, 281, 14256-14262.	1.6	102
21	Camelid nanobodies: killing two birds with one stone. Current Opinion in Structural Biology, 2015, 32, 1-8.	2.6	101
22	Crystal Structure of E.coli Alcohol Dehydrogenase YqhD: Evidence of a Covalently Modified NADP Coenzyme. Journal of Molecular Biology, 2004, 342, 489-502.	2.0	92
23	Structural Characterization and Oligomerization of the TssL Protein, a Component Shared by Bacterial Type VI and Type IVb Secretion Systems. Journal of Biological Chemistry, 2012, 287, 14157-14168.	1.6	91
24	Structural Basis of the Honey Bee PBP Pheromone and pH-induced Conformational Change. Journal of Molecular Biology, 2008, 380, 158-169.	2.0	87
25	Reverse chemical ecology: Olfactory proteins from the giant panda and their interactions with putative pheromones and bamboo volatiles. Proceedings of the National Academy of Sciences of the United States of America, 2017, 114, E9802-E9810.	3.3	86
26	Lateral recognition of a dye hapten by a llama VHH domain. Journal of Molecular Biology, 2001, 311, 123-129.	2.0	85
27	The Insect Attractant 1-Octen-3-ol Is the Natural Ligand of Bovine Odorant-binding Protein. Journal of Biological Chemistry, 2001, 276, 7150-7155.	1.6	80
28	Direct in Vivo Screening of Intrabody Libraries Constructed on a Highly Stable Single-chain Framework. Journal of Biological Chemistry, 2002, 277, 45075-45085.	1.6	80
29	The Crystal Structure of Odorant Binding Protein 7 from Anopheles gambiae Exhibits an Outstanding Adaptability of Its Binding Site. Journal of Molecular Biology, 2011, 414, 401-412.	2.0	76
30	Functional and structural dissection of the tape measure protein of lactococcal phage TP901-1. Scientific Reports, 2016, 6, 36667.	1.6	75
31	A medium-throughput crystallization approach. Acta Crystallographica Section D: Biological Crystallography, 2002, 58, 2109-2115.	2.5	73
32	Structure of Human Pancreatic Lipase-Related Protein 2 with the Lid in an Open Conformation [,] . Biochemistry, 2008, 47, 9553-9564.	1.2	68
33	Structures and host-adhesion mechanisms of lactococcal siphophages. Frontiers in Microbiology, 2014, 5, 3.	1.5	63
34	Crystal structure of a ternary complex between human chorionic gonadotropin (hCG) and two Fv fragments specific for the α and β-subunits 1 1Edited by I. A. Wilson. Journal of Molecular Biology, 1999, 289, 1375-1385.	2.0	62
35	Crystal Structure of the Receptor-Binding Protein Head Domain from Lactococcus lactis Phage blL170. Journal of Virology, 2006, 80, 9331-9335.	1.5	62
36	Queen Bee Pheromone Binding Protein pH-Induced Domain Swapping Favors Pheromone Release. Journal of Molecular Biology, 2009, 390, 981-990.	2.0	62

#	Article	IF	CITATIONS
37	Crystal Structure of the VgrG1 Actin Cross-linking Domain of the Vibrio cholerae Type VI Secretion System. Journal of Biological Chemistry, 2012, 287, 38190-38199.	1.6	60
38	The Atomic Structure of the Phage Tuc2009 Baseplate Tripod Suggests that Host Recognition Involves Two Different Carbohydrate Binding Modules. MBio, 2016, 7, e01781-15.	1.8	58
39	Bivalent Llama Single-Domain Antibody Fragments against Tumor Necrosis Factor Have Picomolar Potencies due to Intramolecular Interactions. Frontiers in Immunology, 2017, 8, 867.	2.2	57
40	The Importance of Framework Residues H6, H7 and H10 in Antibody Heavy Chains: Experimental Evidence for a New Structural Subclassification of Antibody VH Domains. Journal of Molecular Biology, 2001, 309, 701-716.	2.0	55
41	Crystal Structure and Function of a DARPin Neutralizing Inhibitor of Lactococcal Phage TP901-1. Journal of Biological Chemistry, 2009, 284, 30718-30726.	1.6	55
42	Structure and Molecular Assignment of Lactococcal Phage TP901-1 Baseplate. Journal of Biological Chemistry, 2010, 285, 39079-39086.	1.6	55
43	Molecular Insights on the Recognition of a Lactococcus lactis Cell Wall Pellicle by the Phage 1358 Receptor Binding Protein. Journal of Virology, 2014, 88, 7005-7015.	1.5	53
44	Boar salivary lipocalin. FEBS Journal, 2002, 269, 2449-2456.	0.2	52
45	Crystal structure of a novel type of odorant-binding protein from <i>Anopheles gambiae</i> , belonging to the C-plus class. Biochemical Journal, 2011, 437, 423-430.	1.7	52
46	Crystal structures of bovine odorant-binding protein in complex with odorant molecules. FEBS Journal, 2004, 271, 3832-3842.	0.2	51
47	Type VI secretion TssK baseplate protein exhibits structural similarity with phage receptor-binding proteins and evolved to bind the membrane complex. Nature Microbiology, 2017, 2, 17103.	5.9	48
48	Crystal structure of aphrodisin, a sex pheromone from female hamster11Edited by R Huber. Journal of Molecular Biology, 2001, 305, 459-469.	2.0	46
49	The Escherichia coli YadB Gene Product Reveals a Novel Aminoacyl-tRNA Synthetase Like Activity. Journal of Molecular Biology, 2004, 337, 273-283.	2.0	45
50	The crystal structure of the Escherichia coli lipocalin Blc suggests a possible role in phospholipid binding. FEBS Letters, 2004, 562, 183-188.	1.3	45
51	Viral infection modulation and neutralization by camelid nanobodies. Proceedings of the National Academy of Sciences of the United States of America, 2013, 110, E1371-9.	3.3	45
52	Cas9 Allosteric Inhibition by the Anti-CRISPR Protein AcrIIA6. Molecular Cell, 2019, 76, 922-937.e7.	4.5	44
53	Crystal Structure and Self-Interaction of the Type VI Secretion Tail-Tube Protein from Enteroaggregative Escherichia coli. PLoS ONE, 2014, 9, e86918.	1.1	44
54	<scp>X</scp> â€ray structure of a superinfection exclusion lipoprotein from phage <scp>TP</scp> â€ <scp>J</scp> 34 and identification of the tape measure protein as its target. Molecular Microbiology, 2013, 89, 152-165.	1.2	43

#	Article	IF	CITATIONS
55	Structure of the host-recognition device of Staphylococcus aureus phage i•11. Scientific Reports, 2016, 6, 27581.	1.6	42
56	Kinetics and interaction studies between cytochrome c3 and Fe-only hydrogenase fromDesulfovibrio vulgaris hildenborough. Proteins: Structure, Function and Bioinformatics, 1998, 33, 590-600.	1.5	39
57	The targeted recognition of <scp><i>L</i></scp> <i>actococcus lactis</i> phages to their polysaccharide receptors. Molecular Microbiology, 2015, 96, 875-886.	1.2	39
58	Selection, Characterization and X-ray Structure of Anti-ampicillin Single-chain Fv Fragments from Phage-displayed Murine Antibody Libraries. Journal of Molecular Biology, 2001, 309, 671-685.	2.0	36
59	Evolved distal tail carbohydrate binding modules of <scp><i>L</i></scp> <i>actobacillus</i> phage <scp>J</scp> â€1: a novel type of antiâ€receptor widespread among lactic acid bacteria phages. Molecular Microbiology, 2017, 104, 608-620.	1.2	35
60	Neutralization of Human Interleukin 23 by Multivalent Nanobodies Explained by the Structure of Cytokine–Nanobody Complex. Frontiers in Immunology, 2017, 8, 884.	2.2	35
61	The structure of an entire noncovalent immunoglobulin kappa light-chain dimer (Bence-Jones protein) reveals a weak and unusual constant domains association. FEBS Journal, 1999, 260, 192-199.	0.2	34
62	Conserved and Diverse Traits of Adhesion Devices from Siphoviridae Recognizing Proteinaceous or Saccharidic Receptors. Viruses, 2020, 12, 512.	1.5	34
63	Domain swapping of a llama VHH domain builds a crystal-wide β-sheet structure. FEBS Letters, 2004, 564, 35-40.	1.3	32
64	Structure and specificity of the Type VI secretion system ClpV-TssC interaction in enteroaggregative Escherichia coli. Scientific Reports, 2016, 6, 34405.	1.6	31
65	Cryo-Electron Microscopy Structure of Lactococcal Siphophage 1358 Virion. Journal of Virology, 2014, 88, 8900-8910.	1.5	30
66	Camelid nanobodies raised against an integral membrane enzyme, nitric oxide reductase. Protein Science, 2009, 18, 619-628.	3.1	28
67	Crystal Structure of ORF12 from <i>Lactococcus lactis</i> Phage p2 Identifies a Tape Measure Protein Chaperone. Journal of Bacteriology, 2009, 191, 728-734.	1.0	26
68	Structural Mimicry of Receptor Interaction by Antagonistic Interleukin-6 (IL-6) Antibodies. Journal of Biological Chemistry, 2016, 291, 13846-13854.	1.6	24
69	Crystal Structure of a Chimeric Receptor Binding Protein Constructed from Two Lactococcal Phages. Journal of Bacteriology, 2009, 191, 3220-3225.	1.0	22
70	Revisiting the host adhesion determinants of <i>Streptococcus thermophilus</i> siphophages. Microbial Biotechnology, 2020, 13, 1765-1779.	2.0	20
71	Optimization of crystals from nanodrops: crystallization and preliminary crystallographic study of a pheromone-binding protein from the honeybeeApis melliferaL Acta Crystallographica Section D: Biological Crystallography, 2003, 59, 919-921.	2.5	19
72	Structure and Assembly of TP901-1 Virion Unveiled by Mutagenesis. PLoS ONE, 2015, 10, e0131676.	1.1	19

#	Article	IF	CITATIONS
73	Occurrence, integrity and functionality of AcaML1–like viruses infecting extreme acidophiles of the Acidithiobacillus species complex. Research in Microbiology, 2018, 169, 628-637.	1.0	18
74	Inhibition of Type VI Secretion by an Anti-TssM Llama Nanobody. PLoS ONE, 2015, 10, e0122187.	1.1	16
75	Deswapping bovine odorant binding protein. Biochimica Et Biophysica Acta - Proteins and Proteomics, 2008, 1784, 651-657.	1.1	15
76	<i>Lactococcus lactis</i> phage TP901–1 as a model for <i>Siphoviridae</i> virion assembly. Bacteriophage, 2016, 6, e1123795.	1.9	15
77	The thermo―and acidoâ€stable ORFâ€99 from the archaeal virus AFV1. Protein Science, 2009, 18, 1316-1320.	3.1	13
78	Crystal structure of <i>Bacillus subtilis</i> SPP1 phage gp22 shares fold similarity with a domain of lactococcal phage p2 RBP. Protein Science, 2010, 19, 1439-1443.	3.1	12
79	Biochemical and structural characterization of non-glycosylatedYarrowia lipolyticaLIP2 lipase. European Journal of Lipid Science and Technology, 2013, 115, 429-441.	1.0	12
80	Crystallization and Preliminary Diffraction Analysis of the Catalytic Domain of Xylanase Z from Clostridium thermocellum. Journal of Molecular Biology, 1994, 235, 1348-1350.	2.0	11
81	The Baseplate of Lactobacillus delbrueckii Bacteriophage Ld17 Harbors a Glycerophosphodiesterase. Journal of Biological Chemistry, 2016, 291, 16816-16827.	1.6	11
82	Combining somatic mutations present in different <i>in vivo</i> affinity-matured antibodies isolated from immunized <i>Lama glama</i> yields ultra-potent antibody therapeutics. Protein Engineering, Design and Selection, 2016, 29, 123-133.	1.0	10
83	Improved crystallization of the coxsackievirus B3 RNA-dependent RNA polymerase. Acta Crystallographica Section F: Structural Biology Communications, 2007, 63, 495-498.	0.7	8
84	Multiple crystal forms of endoglucanase CelD: Signal peptide residues modulate lattice formation. Journal of Molecular Biology, 1995, 248, 225-232.	2.0	7
85	Insight into odorant perception: the crystal structure and binding characteristics of antibody fragments directed against the musk odorant traseolide. Journal of Molecular Biology, 1999, 292, 855-869.	2.0	7
86	The crystal structure of ORF14 from <i>Sulfolobus islandicus</i> filamentous virus. Proteins: Structure, Function and Bioinformatics, 2009, 76, 1020-1022.	1.5	7
87	Structural Insights into Lactococcal Siphophage p2 Baseplate Activation Mechanism. Viruses, 2020, 12, 878.	1.5	7
88	Anchoring the T6SS to the cell wall: Crystal structure of the peptidoglycan binding domain of the TagL accessory protein. PLoS ONE, 2021, 16, e0254232.	1.1	7
89	Combining site-specific mutagenesis and seeding as a strategy to crystallize `difficult' proteins: the case ofStaphylococcus aureusthioredoxin. Acta Crystallographica Section F: Structural Biology Communications, 2006, 62, 1255-1258.	0.7	6
90	Production, crystallization and X-ray diffraction analysis of a complex between a fragment of the TssM T6SS protein and a camelid nanobody. Acta Crystallographica Section F, Structural Biology Communications, 2015, 71, 266-271.	0.4	6

#	Article	IF	CITATIONS
91	Structure–Function Analysis of the C-Terminal Domain of the Type VI Secretion TssB Tail Sheath Subunit. Journal of Molecular Biology, 2018, 430, 297-309.	2.0	6
92	Crystallization and preliminary X-ray diffraction analysis of protein 14 fromSulfolobus islandicusfilamentous virus (SIFV). Acta Crystallographica Section F: Structural Biology Communications, 2006, 62, 884-886.	0.7	4
93	Structure of odorant binding proteins and chemosensory proteins determined by X-ray crystallography. Methods in Enzymology, 2020, 642, 151-167.	0.4	2
94	Kinetics and interaction studies between cytochrome c3 and Fe-only hydrogenase from Desulfovibrio vulgaris hildenborough. , 1998, 33, 590.		2